Divertor Heat Flux Reduction and Detachment in NSTX

V. A. Soukhanovskii 1), R. Maingi 2), R. Raman 3), R. E. Bell 4), C. Bush 2), R. Kaita 4), H. W. Kugel 4), C. J. Lasnier 1), B. P. LeBlanc 4), J. E. Menard 4), S. F. Paul 4), A. L. Roquemore 4), and the NSTX Team

1) Lawrence Livermore National Laboratory, Livermore, CA, USA
2) Oak Ridge National Laboratory, Oak Ridge, TN, USA
3) University of Washington, Seattle, WA, USA
4) Princeton Plasma Physics Laboratory, Princeton, NJ, USA

E-mail address of main author: vlad@llnl.gov

Abstract: We report the first successful experiments to achieve significant divertor outer strike point (OSP) peak heat flux reduction in H-mode plasmas with high auxiliary heating in a large spherical torus NSTX. A dissipative divertor scenario with D_2 puffing was employed in lower single null plasma configuration with elongation 1.8-2.0 and triangularity 0.4, where typical reference OSP steady-state peak heat flux was measured to be 4-6 MW/m^2 in the 4 MW NBI-heated H-mode phase. Using midplane or divertor D_2 injection at rates R=$(0.14 - 1.1) \times 10^{22}$ particles/s the OSP peak heat flux was reduced by up to 80 % in the radiative high-recycling divertor regime. A further increase in gas puffing rate to 3×10^{22} particles/s produced a partial OSP detachment and an X-point MARFE which degraded the core plasma confinement. On the basis of a two point scrape-off layer model the open divertor geometry and short connection length are identified as factors leading to relatively small radiative and momentum losses in the NSTX divertor.

1. Introduction

High performance plasma discharges with radiative and dissipative divertors have been developed in large aspect ratio tokamaks to address the issues of high divertor heat fluxes and divertor material erosion [1]. Divertor heat load reduction in these regimes is achieved through volumetric momentum and energy dissipative processes, namely the ion-neutral elastic collisions, recombination and radiative cooling. In those experiments the edge radiative and dissipative losses are usually increased by injecting deuterium (D_2) or impurity gases in the plasma scrape-off layer (SOL). Whereas an H-mode scenario with medium-to-small ELMs and partially detached divertor strike points satisfies the steady-state divertor requirements for an ITER-like tokamak [2], achieving acceptable divertor heat fluxes in a high power density spherical torus (ST) based device, such as the Component Test Facility [3], may be challenging. The low aspect ratio magnetic geometry inherently yields plasma configurations with a short connection length, a small divertor plasma volume, and a small plasma-wetted surface, all of which tend to reduce the benefits of the volumetric processes. On a positive side, the ST geometry enables strongly shaped plasmas with a high divertor poloidal flux expansion which can help reduce the heat flux on the divertor surface in a natural way. Dedicated experimental efforts on the National Spherical Torus Experiment (NSTX) are aimed at the development of divertor heat flux mitigation scenarios in 1-6 MW NBI-heated H-mode plasmas, including dissipative divertor and radiative mantle power exhaust [4], divertor heat flux reduction by plasma shaping [5] and divertor lithium coatings [6]. We report the first successful experiments at achieving significant, between 30 and 80 %, outer strike point (OSP) peak heat flux reduction in 4 MW NBI-heated H-mode plasmas using D_2 puffing.

2. Experiment

Divertor heat flux reduction with D_2 puffing was studied in the lower single null (LSN) configuration with the elongation of $\kappa \simeq 1.8 - 2$, triangularity of $\delta \simeq 0.4$, the *drsep*

parameter of -1.5 cm, the ion ∇B drift toward the lower X-point, $q_{95} \simeq 6-7$, the X-point of 15 - 20 cm, and the OSP flux expansion $f_{exp} = 3-4$. This configuration yielded the highest peak OSP heat flux in NSTX: $q \simeq 7-10$ MW/m^2 have been measured in 1 s long 6 MW NBI-heated H-mode plasmas [7]. This experiment was conducted in $B_t = 0.45$ T, $I_p = 0.7$ MA plasmas heated by the 4 MW neutral beam injection (NBI). The core plasma conditions were: $T_e(0) \simeq (0.8-1.2)$ keV, $\bar{n}_e \simeq (3-5)\times 10^{19}$ m^{-3}, $Z_{eff}(0) \leq 1.2-1.4$, with the Greenwald density limit [8] being at $n_G \simeq 5.5\times 10^{19}$ m^{-3}. H-modes were reliably obtained using high field side fueling at a rate of $\Gamma = (2.4-3.8)\times 10^{21}$ s^{-1}. Small, type V [9], and occasional large ($\Delta W/W \simeq 0.10$), type I, ELMs were observed. The L-H power threshold was at 2.0-2.5 MW. The energy confinement time was $\tau_E \simeq 25-40$ ms, being in the range 1.5 - 2 of the the ITER89P confinement scaling factor, a typical performance measure of low δ, κ plasmas in NSTX [10].

The layout of NSTX divertor diagnostics and gas injectors is shown in Fig. 1. Lower divertor radial profiles were recorded by photometrically calibrated visible and infrared cameras [11, 12]. Other diagnostics used in this study were the 20-point Thompson scattering system [13], four chord divertor bolometry system [14], tile-mounted divertor Langmuir probes, and pressure gauges [15].

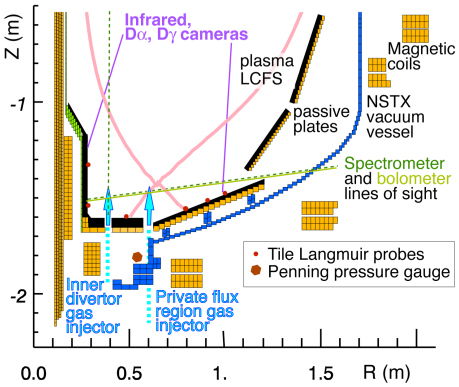

Figure 1: Layout of NSTX divertor diagnostics and gas injectors

Additional quantities of D_2 were injected using the outboard midplane, the inner divertor (ID), and the private flux region (PFR) gas injectors. Both the PFR and the ID injectors were operated at steady-state rates $\Gamma \leq 10^{22}$ s^{-1}. Using a different gas system setup, the ID injector was also operated in a pulsed mode injecting D_2 from four small plenums through four toroidally symmetric ports in the divertor floor. Each pulse duration was 15-20 ms at an average rate of $\Gamma = (0.85-3.0)\times 10^{22}$ s^{-1}. For comparison, the reference plasma particle inventory was in the range $(7-10)\times 10^{20}$.

3. Results

Reference NSTX plasmas demonstrated divertor properties with both similarities and differences from those of conventional tokamak graphite tile clad divertors operating without active pumping [16, 17, 18]. The inner divertor leg detachment occurred naturally at $\bar{n}_e \simeq (2-3)\times 10^{19}$ m^{-3} and input power $0.8 \leq P_{in} \leq 6$ MW. The inner divertor leg region remained in a detached (highly recombining) state with $T_e \leq 1.2$ eV, $n_e \simeq (0.7-4)\times 10^{20}$ m^{-3}, and $q_{in} < 1$ MW/m^2 throughout the operating space [19, 20]. In 1-6 MW NBI H-mode plasmas the outer SOL demonstrated a linear scaling of the peak OSP heat flux q_t with the SOL power, with different slopes at the lower and at the higher P_{SOL}, characteristic of the linear (sheath-limited) and high-recycling (flux-limited) regimes. The peak q_t also increased monotonically with the plasma current [21]. Power balance analysis could typically account for 50-70 % of P_{in}, with 5-10 % radiated in the divertor [14]. The outer SOL did not show any sign of detachment even at the plasma densities approaching the Greenwald limit, with the OSP peak heat flux remaining in the 4-7 MW/m^2 range.

In a dedicated experiment D_2 gas was injected to investigate the effectiveness of the radiative and dissipative techniques for divertor heat load reduction, and the

impact of additional gas puffing on confinement and plasma performance. A general result of adding D_2 injection was a reduction of the peak OSP heat flux by 30-80 %. As the D_2 puffing rate was increased, the outer SOL thermal electron collisionality increased from $\nu_e^* \simeq 5-60$, estimated from the Thomson scattering data at the separatrix in reference plasmas, to $\nu_e^* \simeq 30-80$. The radiative and dissipative SOL losses increased, and the outer SOL transitioned from a radiative high-recycling divertor (RD) regime to a partially detached divertor (PDD) regime [18]. A high-density region with substantial volume recombination, identified as an X-point (divertor) MARFE [22, 23] developed in the vicinity of the X-point at the highest rates of D_2 puffing, shortly before the H-L transition and the core plasma confinement degradation. The operational path to these conditions was different with each gas injector, highlighting the challenge of divertor heat flux reduction in an ST open divertor geometry without active pumping. Puffing D_2 at the midplane in 3 - 4 MW NBI heated plasmas was the least successful as an H-L back transition and large MHD modes occurred within one τ_E, with simultaneous confinement degradation to 0.6-1.0 of the ITER89P scaling. However, the RD and the PDD operating modes, obtained with divertor gas puffing at moderate and high rates, respectively, produced encouraging results described in detail below.

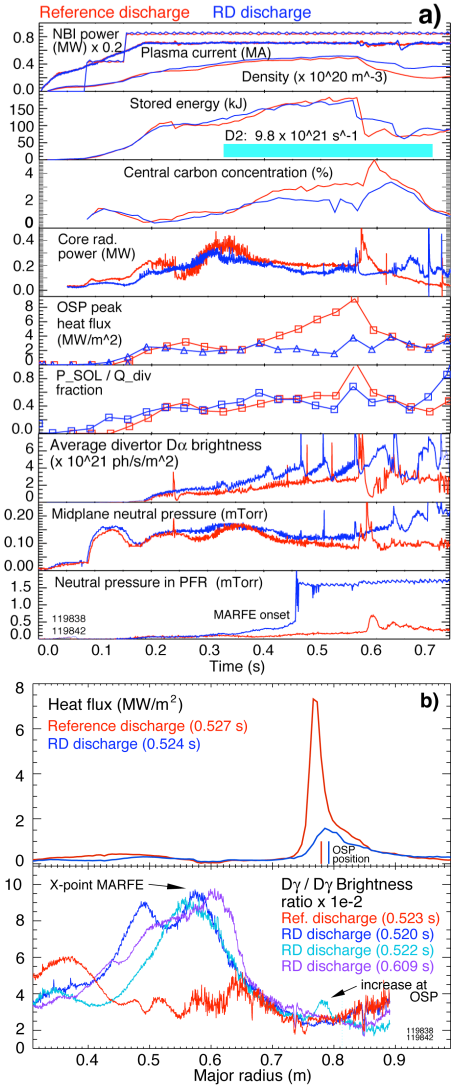

Figure 2: Signal time histories (a) and divertor profiles (b) of a reference and a RD discharges

Radiative high-recycling divertor regime This regime was obtained with a continuous PFR gas injection at rates $(0.3-1.12)\times 10^{22}$ s^{-1}. Shown in Fig. 2 (a) are the time traces of a discharge obtained with the PFR puffing, and a reference plasma. The PFR injection had a modest impact on core plasma parameters: the stored energy, core carbon concentration, electron temperature and density were practically unaffected. H-mode confinement with the ITER89P scaling factor of 1.3-1.6 was retained for about $10\times\tau_E$ with gas puffing, without any change in the ELM regime. The pedestal temperature decreased by 10-20 %, while both the core and the pedestal density increased by 10-30 % during the gas injection phase. The divertor conditions proved to be insufficient for detachment, despite an 40-60 % increase in the divertor radiation and neutral pressure. From the SOL power balance the power loss fraction $(1-Q_{div}/P_{SOL})$ indicated a modest 5-20 % increase due to the gas injection. Here P_{SOL} is the power entering the SOL, determined in the usual manner [14] as $P_{SOL}=P_{NBI}+P_{OH}-dW_{MHD}/dt-P_{rad}^{core}-P_{fast\ ion}^{loss}$, and Q_{div} is an integral of the inner and outer heat flux profiles. The PFR neutral pressure gauge instantaneously

increased and saturated at 0.460 s, indicating the onset of an X-point MARFE, which degraded the core plasma parameters within several τ_E confinement times.

Divertor heat flux and D_2 emission profiles, shown in Fig. 2 (b), supported the above observations. The peak heat flux in the outer divertor was reduced to 1-2 MW/m^2, however, it remained peaked shifting only as a result of strike point drift. A ratio of the divertor D_γ and D_α brightness was previously used to identify the onset and the spatial extent of volume recombination, often indicative of divertor detachment [24]. Here the ratio in the outer divertor region remained similar to that of the reference discharge throughout most of the gas injection phase. As the density increased to $(0.8-0.9)\times n_G$, the D_γ/D_α brightness ratio in the OSP region transiently increased by 2-3 (as shown in Fig.2 (b)), indicating an increase in the volume recombination rate and an imminent transition to a PDD regime. The ratio also increased in the inner divertor and below the X-point region to 0.1, a sign of strong volume recombination [24].

The RD regime appears to be a promising scenario for long-pulse H-mode discharges in NSTX as it combines good plasma performance with a significant heat flux reduction. However, the operational space of the RD regime is limited because only a limited fraction of power can be exhausted by volumetric processes in a high-recycling divertor regime [25], and because of the confinement limitations imposed by the X-point MARFE onset.

Partially detached divertor regime The PDD regime was established by puffing D_2 in a sequence of four D_2 pulses from toroidally symmetric ID gas injectors at a high puffing rate. Shown in Fig. 3 (a) are the time traces of a reference H-mode plasma discharge and a PDD discharge. The gas injection started at 0.250 s. The gas puffing phase was characterized by a strong degradation of core plasma parameters: while the core radiated power and core carbon concentration did not change, the plasma stored energy decreased by 15-25 %, and the pedestal temperature and density decreased by 5-30 %. This discharge transitioned back to L-mode within one τ_E, whereas other

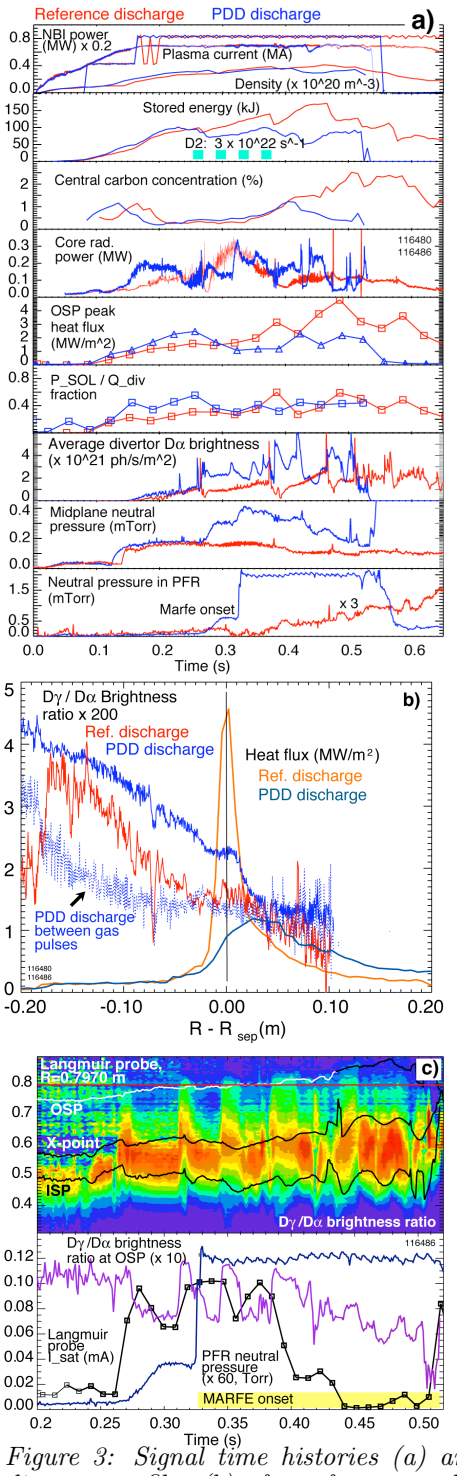

Figure 3: Signal time histories (a) and divertor profiles (b) of a reference and a PDD discharges. Panel (c) compares the D_γ/D_α ratio contour plot with Langmuir probe I_{sat} and PFR neutral pressure time histories

discharges with less gas puffing or a wider separation between individual gas pulses back-transitioned within $(2-7)\times\tau_E$. The ITER89P scaling values during the strong gas puffing were in the range 0.6-1.1. The midplane separatrix temperature remained in the 10-30 eV range; the separatrix density increased by 50-80 %, resulting in an increase in the SOL collisionality to 60-80. The outer divertor peak heat flux remained at 1-2 MW/m^2 throughout the discharge. The SOL power loss fraction was in the range 0-25 %, suggesting that the onset of the PDD regime in NSTX depends on both the momentum loss channel and the radiated power loss channel.

Divertor profiles during the PDD phase, shown along with the reference discharge profiles in Fig. 3 (b), were different from those obtained in the RD regime. The peak heat flux decreased by 65-80 %, the peak moved outward by up to 5 cm, exceeding the OSP natural drift distance, and the profile broadened. Transient onset of volume recombination in the OSP region during the gas pulses was evident from the 50 % increase in the D_γ/D_α brightness ratio. The volume recombination zone was localized to 2-3 cm in the vicinity of the OSP, where the heat flux profile was substantially reduced. The D_γ/D_α ratio values measured at the OSP in the PDD discharges were close to those measured in the detached inner divertor, even though the absolute values were low apparently due to a systematic measurement error.

The spatial dynamics of the volume recombination region in the PDD discharge is compared in Fig. 3 (c) with other divertor diagnostics. An increase of the D_γ/D_α ratio in the region $R=0.40-0.55$ m prior to the gas injection indicated the onset of volume recombination and detachment of the inner divertor leg. With each gas pulse, a region of volume recombination moved up along the inner divertor leg to the X-point, expanded and reached the OSP region. Importantly, correlated with the gas pulses and onset of volume recombination was the decrease of the ion saturation current of the Langmuir probe located at $R=0.7970$ m. The X-point MARFE developed following the second gas pulse at 0.315 s, and slowly moved between the inner strike point and the X-point.

Maintaining a low midplane neutral density and a high divertor neutral density below the MARFE critical value simultaneously is highly desirable for an H-mode reduced divertor heat flux operation [26, 27, 28]. In NSTX the D_2 compression ratio, defined as a ratio of the PFR and midplane neutral pressures, $\eta = p_{div}/p_{mid}$, was in the range 1 - 10, typical for an open divertor geometry with high gas conductance between the divertor and the midplane regions. Shown in Fig. 4 are p_{div} and p_{mid} as a function of density $\bar{n}_e$ in the reference, RD and PDD discharges. The ID gas puffing significantly affected the midplane pressure leading to the loss of H-mode within several confinement times. The reference and the RD plasmas indicated weak dependence of the midplane pressure on density. In all discharges with gas puffing the X-point MARFE onset was closely coupled to the local divertor neutral pressure and less so to the core plasma parameters, similarly to tokamak MARFE observations [29]. The X-point MARFE developed when the midplane pressure was in the range 0.15-0.3 mTorr and the plasma density was

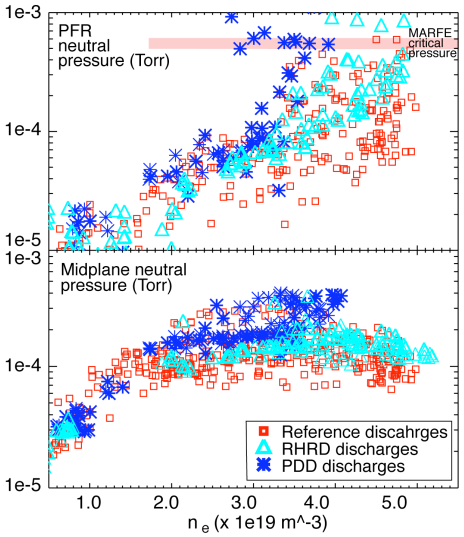

Figure 4: Neutral pressure in the PFR (a) and midplane (b) regions in reference, RD, and PDD discharges

$(0.65 - 0.80) \times n_G$. The PFR pressure in reference discharges increased linearly with density, and came close to the critical MARFE pressure as $\bar{n}_e$ approached the n_G value. The critical MARFE pressure in the PFR was reached faster with high rate puffing from the ID gas injector than from the moderate rate PFR gas injector. The critical PFR neutral pressure for the MARFE onset was 0.5-0.6 mTorr. The PFR pressure was measured by a Penning gauge located 20-30 cm below divertor tiles, therefore, the actual PFR pressure may have been higher. The measured MARFE critical pressure was a factor of 5-8 lower than that reported in the tokamak divertor experiments [29]. As the MARFE developed the PFR pressure increased beyond the Penning gauge saturation limit of 2 mTorr.

4. Discussion

On the basis of tokamak experiments conducted in an open divertor geometry with and without active pumping [16, 17, 18, 26, 27, 28], as well as numerical modeling results for NSTX [19], it was expected that the OSP detachment threshold in $\bar{n}_e$ in the low κ, δ LSN configuration would be high. An open geometry divertor has a reduced ability to re-capture recycling neutrals and maintain high divertor neutral density essential for efficient power and ion momentum dissipation. Active divertor pumping is needed to maintain divertor neutral and plasma density below the critical density of the X-point MARFE onset. Simultaneously, high divertor electron density and/or high impurity concentration are needed for an efficient radiated power exhaust. We have demonstrated that the conventional tokamak divertor heat flux mitigation techniques, such as the radiative and dissipative divertors, are applicable to NSTX. However, our results point to several challenging issues which we discuss below using the two point SOL model with parameterized losses [25, 30, 31]. The question is whether the required SOL power loss fraction f_p and the parallel momentum (pressure) loss fraction f_m can be effectively obtained in NSTX. Here the power loss fraction f_p is due to impurity and hydrogenic radiation and charge exchange, whereas f_m is due to charge exchange, recombination and elastic collisions.

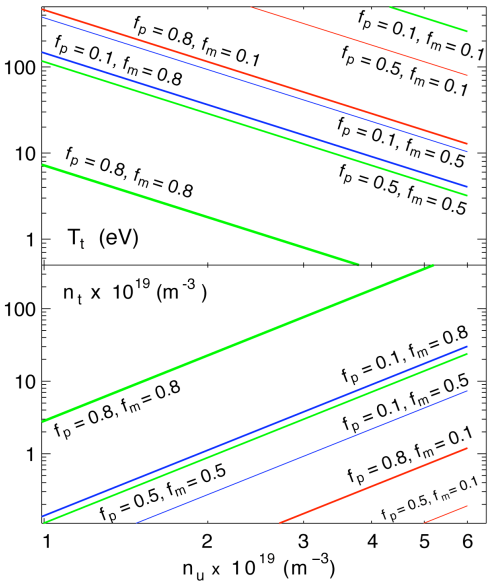

Figure 5: Divertor T_e and n_e calculated from 2PM with parameterized power loss f_p and momentum loss f_m fractions

Shown in Fig. 5 are the calculated divertor density and temperature as a function of the upstream density n_u and f_p, f_m as parameters for a reference H-mode discharge. The conducted power fraction is taken as $f_{cond} = 0.9$, whereas the parallel heat flux $q_{||} = P_{SOL}/A_{SOL} \simeq 3$ MW / 0.1 m^2 = 30 MW/m^2 and the connection length $l_c \simeq 20$ m are determined from the measured quantities. The calculations show that substantial f_p and f_m are necessary to achieve high divertor n_e and low divertor T_e. The momentum loss becomes appreciable only at $T_e \leq 10$ eV [31]. At the typical NSTX separatrix temperatures $T_u \simeq 10 - 30$ eV, low T_t and high $n_t \simeq (5 - 10) \times n_u$ would be obtained with the momentum loss factor $f_m = 2n_t T_t / n_u T_u \simeq 0.5 - 0.8$, a challenging task in the open divertor geometry.

The two point model does not contain the exact cross-field transport physics; the

NSTX specifics are manifested through the higher $q_{||}$, and lower l_c (a result of a low aspect ratio configuration). We now discuss the role of a connection length l_c in the SOL radiated power and momentum loss rate in the NSTX low κ, δ configuration. Shown in Fig. 6 is l_c as a function of a major radius (poloidal flux) at the divertor for a reference. Because of the high magnetic field shearing rate l_c decreases from 15-20 m at the separatrix to about 3-4 m within a radial distance of a few cm at the divertor. The volumetric power loss P_{vol} is determined in part by the flux tube length within the radial region defined by λ_q and λ_n, the SOL power and density decay lengths. Since f_p and f_m are not independent, we estimate the maximum power fraction which is not lost by conduction and which can be radiated. The maximum volumetric power fraction dissipated in the divertor $f_{imp} = 1 - f'_m\ (q_t + q_{Hrad})/q_{||}$, where q_t is the target parallel power flux density and q_{Hrad} is the power loss due to hydrogenic radiation [31]. In the high recycling regime without any momentum loss ($f'_m = 1$) at $T_t = 1 - 10$ eV and $n_u \simeq 1 \times 10^{19}$ m^{-3} the maximum fraction is limited in NSTX to about 0.65-0.75, while in the cases with $f'_m = 0.8 - 0.1$ ("detaching") this fraction is in the range $0.70 - 0.95$. According to the analytic impurity radiated power models from Refs. [32, 33], power flux densities up to 7 MW/m^2, or about 25 % of $q_{||}$, can be radiated by carbon ions in the SOL with $T_u \simeq 10 - 30$ eV. A much longer l_c in the separatrix region, therefore, would promote a partial strike point detachment over a full detachment, and/or an X-point MARFE formation, both of which being critically dependent on the power balance between $q_{||}$ and P_{vol}.

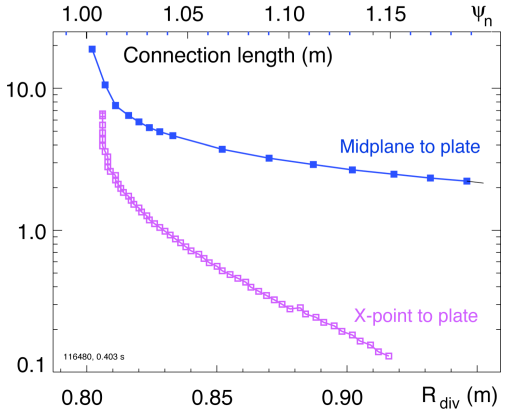

Figure 6: Midplane-to-plate and X-point-to-plate connection lengths as a function of major radius (normalized poloidal flux) at divertor floor

The connection length also impacts the parallel momentum removal process. The energy and momentum removal rate due to the volume recombination process may be substantially reduced in short flux tubes. In an electron-ion recombination process, for a thermal ion with $v \simeq 10^4$ m/s the divertor residence time would be $\tau_{ion} = l_d/v \leq 0.8$ ms. Here l_d is the X-point to target connection length, shown in Fig. 6. The recombination time at $T_e \leq 1.3$ eV is $\tau_r = 1./(n_e R_{rec}) \simeq 1 - 10$ ms [32], making it marginally possible for an ion to recombine in the longer flux tubes, and not possible in the shorter ones, unless a very high divertor density n_e is sustained.

The given physical arguments provide an explanation of why the SOL power and momentum loss factors appear to be relatively small in the low κ, δ LSN configuration in NSTX. Numerical modeling with a two-dimensional multi-fluid edge transport code UEDGE will allow a better evaluation of their relative contributions [34].

Summary

Dedicated divertor heat flux reduction experiments have been conducted in 4 MW NBI heated H-mode plasmas in a low δ, κ LSN configuration using divertor D_2 injection. A high-recycling radiative divertor operation has been demonstrated at moderate gas puffing rates and a transient partial detachment of the outer strike point was obtained at high gas puffing rates. Gas puffing led to a development of a stable X-point MARFE, and degraded the plasma confinement at the highest puffing rates. The peak heat flux

was reduced 50-80 % to an acceptable level of 1-2 MW/m^2 in both cases. A radiative high-recycling divertor regime may be a more viable option for divertor heat flux reduction in moderately shaped NSTX plasmas as the short parallel connection length and the open divertor geometry reduce the effectiveness of the volumetric radiative and dissipative processes. Future experimental work will focus on divertor characterization in highly shaped LSN and DN configurations, and characterizing the effects of lithium coatings [6] on divertor operation.

Acknowledgements

This research was supported by the U.S. Department of Energy under contracts No. W-7405-Eng-48, DE-AC02-76CH03073, DE-AC05-00OR22725, and W-7405-ENG-36.

References

[1] ITER PHYSICS EXPERT GROUP ON DIVERTOR et al., Nuc. Fusion **39** (1999) 2391.
[2] POST, D. et al., Phys. Plasmas **4** (1997) 2631.
[3] PENG, Y.-K. et al., Plasma Phys. Control. Fusion **47** (2005) 263.
[4] SOUKHANOVSKII, V. A. et al., at press, J. Nucl. Mater. (2007).
[5] GATES, D. A. et al., Phys. Plasmas **13** (2006) 056122.
[6] MAJESKI, R. et al., Paper EX/P4-23 (this conference).
[7] MAINGI, R. et al., Plasma Phys. Control. Fusion **45** (2003) 657.
[8] GREENWALD, M., Plasma Phys. Control. Fusion **44** (2002) R27.
[9] MAINGI, R. et al., Phys. Plasmas **13** (2006) 092510.
[10] MAINGI, R. et al., Nuc. Fusion **43** (2003) 969.
[11] MASTROVITO, D. et al., Rev. Sci. Instrum. **74** (2003) 5090.
[12] SOUKHANOVSKII, V. A. et al., Rev. Sci. Instrum. **74** (2003) 2094.
[13] LEBLANC, B. P. et al., Rev. Sci. Instrum. **74** (2003) 1659.
[14] PAUL, S. et al., J. Nucl. Mater. **337-339** (2005) 251.
[15] RAMAN, R. et al., Rev. Sci. Instrum. **75** (2004) 4347.
[16] ALLEN, S. et al., Nuc. Fusion **39** (1999) 2015.
[17] PETRIE, T. et al., J. Nucl. Mater. **196-98** (1992) 848.
[18] PETRIE, T. et al., Nuc. Fusion **37** (1997) 321.
[19] SOUKHANOVSKII, V. et al., J. Nucl. Mater. **337-339** (2005) 475.
[20] SOUKHANOVSKII, V. A. et al., Rev. Sci. Instrum **77** (2006) 10F122.
[21] MAINGI, R. et al., at press, J. Nuc. Mater. (2007).
[22] LIPSCHULTZ, B., J. Nucl. Mater. **145-147** (1987) 15.
[23] PETRIE, T. et al., J. Nucl. Mater. **241-243** (1997) 639.
[24] MCCRACKEN, G. M. et al., Nuc. Fusion **38** (1998) 619.
[25] BORRASS, K. et al., Nuc. Fusion **34** (1994) 1203.
[26] ALLEN, S. et al., Plasma Phys. Control. Fusion **37** (1995) 191.
[27] PETRIE, T. et al., Nuc. Fusion **37** (1997) 643.
[28] ALLEN, S. et al., J. Nucl. Mater. **266** (1999) 168.
[29] GHENDRIH, P. et al., J. Nucl. Mater. **220-222** (1995) 305.
[30] STANGEBY, P. C., *The plasma boundary of Magnetic Fusion Devices*, IoP, Bristol, 2000.
[31] PITCHER, C. et al., Plasma Phys. Control. Fusion **39** (1997) 779.
[32] POST, D. et al., J. Nucl. Mater. **220-222** (1995) 1014.
[33] MONIER-GARBET, P. et al., J. Nucl. Mater. **266 - 269** (1999) 611.
[34] RENSINK, M. E. et al., J. Nucl. Mater. **290-293** (2001) 706.